COBEM 2023 27TH INTERNATIONAL CONGRESS OF MECHANICAL ENGINEERING

ABCM Brazilian Society of Mechanical Sciences and Engineering
27th ABCM International Congress of Mechanical Engineering
December 04-08, 2023, Florianópolis-SC, Brazil

COB-2023-1053
COMPARATIVE SURFACE ANALYSIS AND SOLUTIONING THERMOCOUPLE INTERNAL POSITION PROBLEM OF VERTICAL HEAT EXCHANGER TUBES USED IN THE FALLING FILM EVAPORATION PROCESS

Patrick Walter Rüdiger Scheidt
Arthur Kleyton Azevedo de Araújo
Universidade Federal de Santa Catarina, Departamento de Engenharia Mecânica patrickwrscheidt@gmail.com and arthurkleyton@gmail.com

Jessé Steinert Barbiaro
Universidade Federal de Santa Catarina, Departamento de Engenharia Mecânica jessesteinbar@gmail.com

Tainan Daniel Andrioni
Universidade Federal de Santa Catarina, Departamento de Engenharia Mecânica tainan.andrioni@labmat.ufsc.br

Rafael dos Santos Maximo
Universidade Federal de Santa Catarina, Departamento de Matemática maximo.rafael13@gmail.com

Júlio César Passos
Universidade Federal de Santa Catarina, Departamento de Engenharia Mecânica julio.passos@lepten.ufsc.br

The heat exchanger tubes used in the falling film evaporation process have gained significant attention due to their high efficiency in separating liquid mixtures. This process is widely used in different industry fields such as food, beverage, dairy, chemical, pharmaceutical and even nuclear. The flow of a thin liquid film over a heated surface causes evaporation and concentration of the remaining solute, making it ideal for heat-sensitive and viscous products that may degrade due to temperature. Falling film evaporators are highly customizable and can be designed to meet specific process requirements, which make them more efficient than other separation techniques. This study aims to analyze the surfaces of the modified heat exchanger tubes used in falling film evaporation and propose an alternative to attach thermocouples to the inner wall of the exchanger for future thermal analysis testing. The researchers used interferometry to obtain topographic parameters and images via MountaisMap software. The results demonstrate that the topographical parameters Sa (arithmetical mean height), Sq (root mean square height), and Sz (maximum height) on the grooved surface are approximately four times higher than those on the tube's external wall. The volume of the motifs obtained in the groove is about three and a half times greater than that of the external wall, which can significantly affect the evaporation process in this area. In order to fix the thermocouples in place, the researchers designed and 3D printed a rod that conducts the thermocouples to the desired positions in the internal wall. This solution may enable accurate thermal analysis of the falling film evaporator, which makes it more efficient and reliable. With the increasing demand for energy-efficient separation techniques, falling film evaporation is gaining more attention in different industry sectors. Understanding the surfaces of modified heat exchanger tubes and accurately monitoring their thermal behavior for optimizing the process and improving efficiency is crucial.

Keywords: *Falling Film Evaporator, Vertical Tube, Surface, Thermocouple*

1. INTRODUCTION

Boiling is the physical phenomenon of phase transition from liquid into gas when heat is supplied, and the liquid reaches its boiling point. However, even though evaporation involves the same change of physical state, this process is usually slower and occurs gradually, depending on a specific temperature and pressure. Moreover, evaporation takes place at the fluid's surface without forming bubbles, unlike boiling.

Studies focusing on Falling Film Evaporation (FFE) have primarily started due to the need for optimizing thermal efficiency, space, and cost in industrial facilities. In Brazil, since the 70s, theses on FFE in the context of the dairy industry have been defended. Zhang, Ma, and Zhang (2021) highlight that the majority of studies undertaken on heat exchangers using the FFE phenomenon focus on horizontal tubes. Thus, there are gaps in understanding the characteristics of FFE in vertical tubes, specifically regarding the behavior of the films outside the tubes. Therefore, this requires further investigations. Köroğlu, Lee, and Park (2013) mention that surface modifications of heat exchangers can significantly improve wettability and heat transfer rate. These modifications can be made chemically at nanoscale or through coarser mechanical alterations through machining processes.

In this sense, the present study aims to analyze the surfaces of the modified heat exchanger tubes used in falling film evaporation and propose a solution for attaching thermocouples to the inner wall of the exchanger for future thermal analysis testing. This analysis is part of a study that seeks to investigate the effect of surface type, smooth or grooved, on the heat transfer coefficient during the FFE process on the external surface of an internally heated vertical tube. This study also seeks to contribute with solutions to issues regarding assembly and fixing of thermocouples, as well as obtaining topographical results of the heat exchangers based on the surface type.

1.1. Falling Film Evaporation

The FFE process is a physical phase change phenomenon that occurs at the liquid-vapor interface when a liquid film is heated. This film flows over a surface under the influence of gravity along the heated region. Heat exchangers that utilize the FFE process can be constructed in different formats, usually tubular or flat plates. The FFE phenomenon has been employed in processes in order to separate volatile components present in mixtures. Thus, the use of thin liquid films occurs in industrial process equipment where heat and mass transfer phenomena take place (Wang et al., 2010; Gourdon et al., 2015; Huang; Yang; Hu, 2015).

Silveira (2015) summarizes that the process consists of a thin liquid film flowing downward — after passing through a distributor and being preheated close to the evaporation temperature — in order to be partially evaporated. In this sense, the main independent parameters ruling the heat transfer process in the FFE phenomenon are: 1. boiling temperature; 2. temperature difference (ΔT) between the temperatures of the heated surface and the liquid; 3. flow rate of the liquid falling over the heated surface; 4. initial temperature of the liquid, just before it comes into contact with the heated surface; 5. concentration of the liquid in the evaporator in the case of mixtures; 6. geometry and orientation of the main elements of the heat exchanger where the process occurs; 7. characteristics of the heat exchanger elements such as material type, surface treatments, and thickness (Chen; Jebson, 1997).

According to Ji et al. (2019), FFE is one of the most efficient heat transfer processes. Furthermore, Ribatski and Jacobi (2005) also emphasize that implementing heat exchangers that utilize the FFE phenomenon compared to other existing options such as pool boiling scenarios reduces cost. The size reduction of the heat exchanger, combined with the low fluid inventory required in this process, is extremely beneficial in terms of cost and space utilization. FFE heat exchangers can operate with fluids of different concentrations and viscosities.

1.2. FFE Applications

One of the earliest patents for falling film evaporators was registered in 1888 (Lyle, 1947). However, before 1970, there were not many researchers involved in the field until its use was applied in ocean thermal energy conversion (OTEC) systems in the 1970s. Such application revived, still within this field, in the 1980s due to the second global oil crisis. However, it was only in the 1990s that the FFE process became widespread due to the elimination of CFCs motivated by the Montreal Protocol, a global agreement signed in 1987 aimed at protecting the ozone layer. Although these evaporators have advantages in refrigeration and air conditioning applications, they are not currently used in these applications on a global scale due to complications with non-uniformity of the liquid film (Abed et al., 2015).

Food industries commonly use multi-stage evaporators, which often utilize falling film evaporators in various configurations, such as vertical tubes with internal or external flow, corrugated plates, horizontal tubes with external flow, etc. In the dairy industry, multi-stage evaporators typically have long vertical tubes with external flow in their plants for the production of powdered products (Gourdon et al., 2015).

Flavonoids, proteins, and other organic compounds responsible for the flavor and integrity of food can degrade relatively easily when exposed to certain amounts of heat (Zhang et al., 2019; Dumpler; Huppertz; Kulozik, 2020). In this sense, as FFE heat exchangers operate at low thermal fluxes, the use of these equipment allows for a better quality of the final product (usually dairy or fruit juices), as the heat-induced denaturation is minimal. As active compounds from plants often require solvents for their extraction, the use of the Falling Film Evaporation (FFE) process may be employed in the subsequent step, where the solvent must be evaporated in order to leave only the medicinal compounds (Leheng Chemical Equipment Manufacturing, 2022). Due to the low heat flux used, the integrity of organic compounds present in herbal medicine is preserved. Additionally, falling film heat exchangers can operate with high viscosity fluids, allowing for the processing of more viscous oils.

According to the Chinese company Wuxi Chemical Equipment (2022), Falling Film Evaporation (FFE) is widely used in petrochemical industry plants in the production of glycol, ethanolamine, caprolactam, styrene, alkylphenols, acrylic fibers, polyester, polycarbonate, among others. This way, compared to traditional equipment, heat exchangers using FFE have provided a 40% increase in heat transfer efficiency and a 30% reduction in energy consumption. It is worth noting that in 2018, the FFE technology developed by the company was assessed by the Chinese Petroleum and Chemical Industry Association, breaking the international monopoly and being nationally acknowledged for technological advancement (Wuxi Chemical Equipment, 2022).

After the nuclear accident in Fukushima back in 2011, safety-oriented research in the sector has drawn significant attention over the last decade. In the AP1000 nuclear power plants developed by the American company Westinghouse Electric Company, Falling Film Evaporation (FFE) in countercurrent flow with an air stream is the primary method for removing heat from the Passive Containment Cooling System (PCCS) (Huang; Yang; Hu, 2015; Wang et al., 2016; Hu; Hu, 2021).

There are around twenty thousand desalination plants worldwide today. These plants can provide potable water or reused water in locations where there are no accessible aquifers or rivers. Additionally, in some countries, more than 90% of their total water supply comes from this process (AQUATECH, 2019). A wide array of new methods have been developed over time for desalinating seawater, the main ones being multiple-stage flash distillation, reverse osmosis, and low-temperature multi-effect distillation (LTMED) (Shen et al., 2013). According to Shen et al. (2013), FFE in horizontally arranged tubes is the preferred LTMED technique by industries to desalinate seawater. This is because it reduces maintenance costs due to lower corrosion rates. Furthermore, Hou, Bi, and Zhang (2012) highlight that this technology is promising as it provides the operation with large amounts of water and enables high heat transfer with low temperature differences.

2. MATERIALS AND METHODS

This section aims to provide a detailed overview of all techniques, materials, and methods used in this study. It provides a thorough explanation of the experimental setup, including its main features, instrumentation, and procedures. It presents the process of solving the internal thermocouple positioning problem and the methodology for processing the topographic data as well.

2.1. Stainless steel AISI 304 heat exchanger tubes

The stainless steel AISI 304 tubes were manufactured with internal gaps in order to have the thermocouples inserted inside. The dimensions of the tubes are: tube length (L_{tube}) = 100 mm and tube diameter (D_{tube}) = 31.5 mm. The resistance responsible for the heating is placed in its cylindrical overlap, with a diameter (Ø) of 19 mm. Furthermore, these tubes allow the fitting of the distributor, which is made of Polytetrafluoroethylene (Teflon), at their upper end. Figure 1 shows the tube without surface modifications (a) and the modified tube (b).

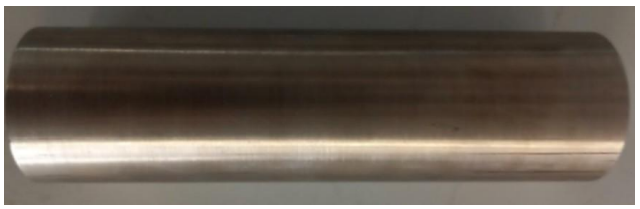

Figure 1. Stainless steel AISI 304 tube (a) without grooves.

(b). Stainless steel AISI 304 tube with grooves.

2.2. Positioning and fixation of thermocouples on the inner wall of the tube

One of the main challenges of this work was the positioning and fixation of the thermocouples in the gaps, which are spaced 120º apart inside the tube. The number of thermocouples in each gap, the precision of their relative positions, and the need to ensure contact with the inner wall make it difficult to fix them correctly. Figure 2 brings a sketch showing the path and positioning points of the thermocouples. To solve this problem, a curved passage rod was fabricated using 3D resin printing. Figure 3 (a) and (b) shows its technical drawing views. These passages serve to guide the thermocouples and ensure their contact in the correct positions on the inner wall of the tubes. Three rods are used per tube in total.

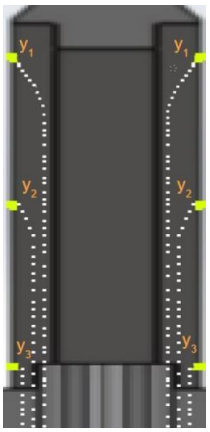

Figure 2. Sketch of the path and positioning points of the thermocouples.

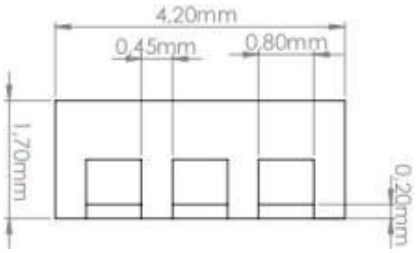

Figure 3 (a). Technical drawing front view

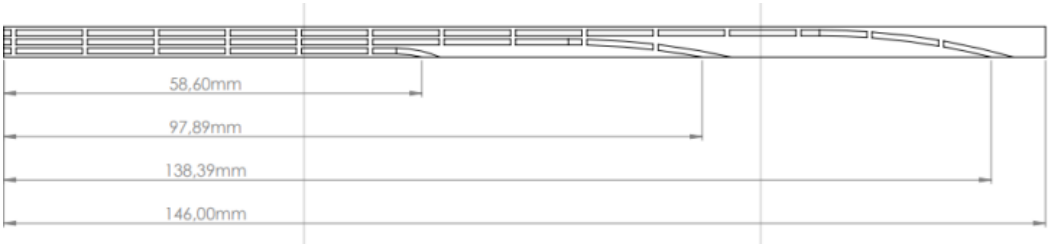

Figure 3 (b). Technical drawing top view

Figure 4 shows the Anycubic Photo Mono X resin 3D printer that was used to manufacture this rod. The use of this equipment was the cost reduction for prototyping and validating the functionality of the rod. The resin used was the Poseidon Washable Grey Resin from Quanton 3D. Since it is washable, there would be no problem with water flow damaging it or being solubilized in the system.

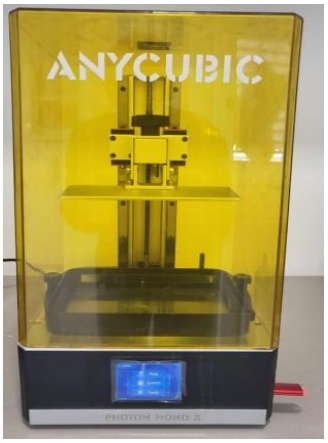

Figure 4. Anycubic Photo Mono X 3D Printer

2.3. Treatment of topographic data

The present study conducted imaging of the topography of the smooth wall surface and the groove present in the heat exchanger tube. Thus, there is the possibility of additional analysis that allows for correlations and further investigation, both in the present work and in future studies, based on data from the obtained parameters.

The equipment used for acquiring topographic data, as shown in Figure 5, was the Zygo NewView 7300 interferometer, available at the Federal University of Santa Catarina (UFSC)'s Materials Laboratory (LabMat). The data processing was performed using the MountainsMap software. This processing is required in order to split the surface into its three components: shape, waviness, and roughness. Consequently, it enables the calculation of peak and valley amplitudes and intensities, which together constitute the roughness. The significance of this information is directly linked to wettability, as these factors are correlated with the surface property of the material.

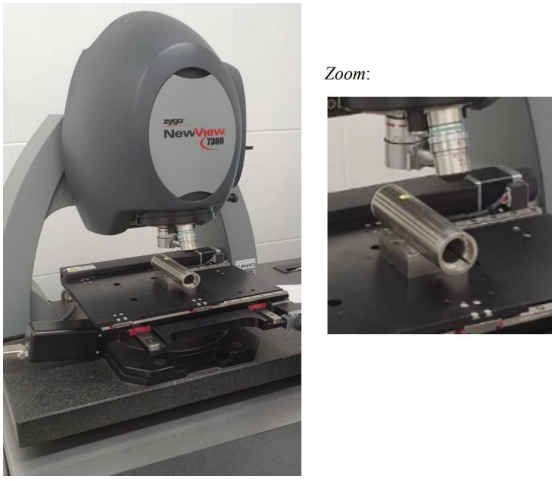

Figure 5. Zygo NewView 7300 Interferometer

Firstly, the unmeasured points need to be filled. These points regularly appear in interferometer operations due to various factors, including pores, peaks with steep slopes where waves reflect and do not return to the detector, and significant differences in reflectivity between phases of the analyzed material.

After the points have been filled, a second-degree polynomial removal tool is used to eliminate the form. Then, the waviness is filtered to isolate the roughness for analysis. The cut-off used was 0.25 mm, following the ISO 4288:1996 standard. Consequently, the software considers repeating patterns with wavelengths greater than 0.25 mm as waviness, while those below this value are filtered as part of the roughness. Finally, the software allows the projection of three-dimensional images of roughness, waviness, and form. This enables visual analysis of the investigated surfaces. Moreover, the topographic parameters explained in the following section are also presented.

2.3.1. Relevant topographic parameters

Topographic parameters are a way to approach and understand a surface mathematically, and also enables an understanding of the distribution of irregularities across a three-dimensional topography. Two widely used parameters in surface characterization are *Sa* (arithmetic mean) and *Sq* (root mean square of *Sa*). The values of *Sa* and *Sq* tend to increase when a surface exhibits large amplitude, representing the difference between the highest peaks and the deepest valleys. *Sz* is also a relevant parameter that represents the maximum height of the highest peak. The MountainsMap software calculates all the parameters mentioned above, and also computes motifs, which provide the volumetric area of cavities below a specific cut-off.

3. RESULTS AND DISCUSSION

This section aims to present, in a direct and objective manner, the analysis of the surface topography of the tubes by providing a 3D visualization of the smooth wall and the grooved surface. This allows for an analysis of the relevant topographic parameters for this and future studies involving the FFE process. Furthermore, the solution for the positioning and fixation of thermocouples onto the inner wall of the tube is presented.

3.1. Topographic analysis of the tubes

The results presented in this section will be divided into two parts: the first will address the 3D axonometric projections, whereas the second will deal with the presentation of roughness profiles and analysis of topographic parameters.

3.1.1. Axonometric projections

3.1.1.1. Surface axonometric projection

The surface shown in Figure 6 displays the surface axonometric projection (SAP) of the smooth wall of the tube. First, one can observe the characteristic sanding marks. In this image, the cylindrical shape of the wall can be seen, which clarifies its dimensional variation in the Cartesian axes.

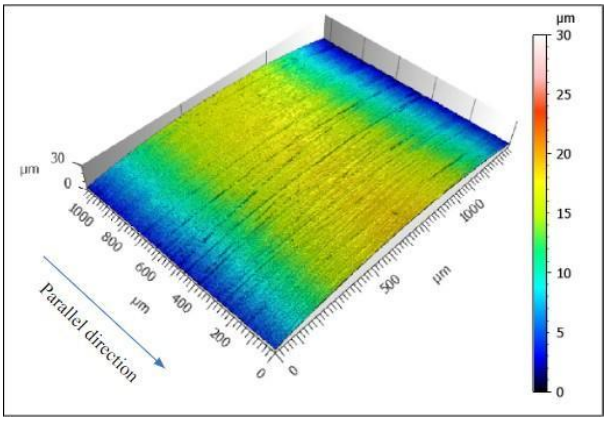

Figure 6. SAP of the smooth wall

The axonometric projection shown in Figure 7 corresponds to the surface axonometric projection of the groove. It is possible to observe that the relief is lower at the edge. This is due to the electroerosion process, where electric charges tend to concentrate at the corners, resulting in the removal of a greater amount of material.

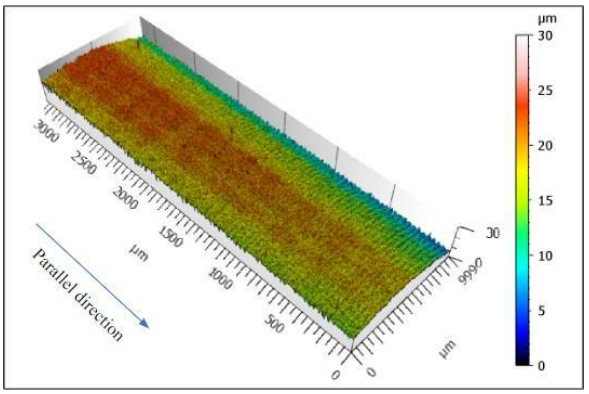

Figure 7. SAP of the groove

3.1.1.2. Roughness axonometric projection

Figures 8 (a) and (b) show, respectively, the roughness axonometric projection (RAP) of the smooth wall and the groove. From the images, by reading and interpreting values, the roughness peaks of the groove are more prominent compared to those of the smooth wall. The machining process to which each surface was subjected aligns with the obtained images.

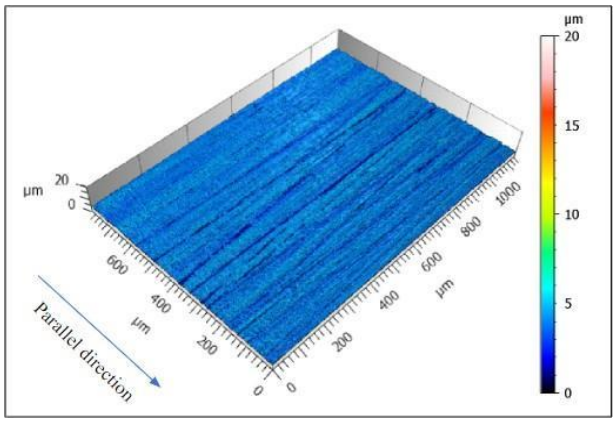

Figure 8 (a). RAP of the smooth wall

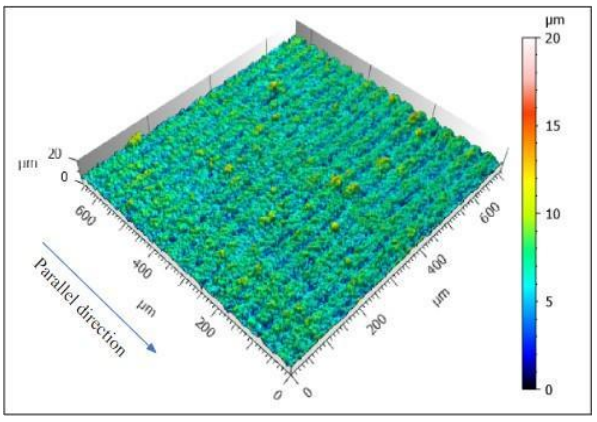

(b). RAP of the groove

3.1.2. Analysis of roughness profiles and topographic parameters

3.1.2.1. Smooth wall

The roughness profiles were traced parallel and perpendicular to machining passes. Figures 9 and 10 below show the profiles of the smooth wall. The figures show no expressive difference between both profiles, which suggests that the sanding process was well executed to standardize the smooth wall surface.

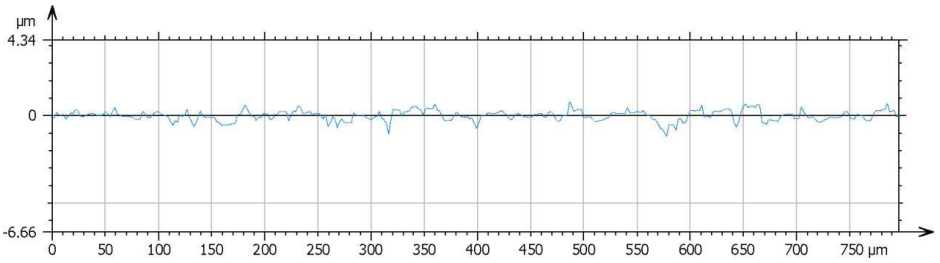

Figure 9. Profile 1, parallel to machining passes

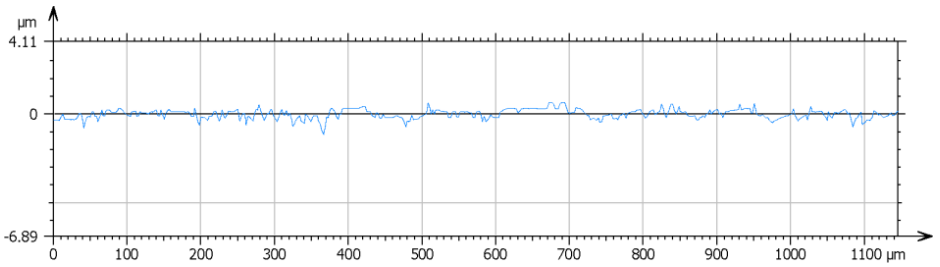

Figure 10. Profile 2, perpendicular to machining passes

The topographical parameters obtained in the data collection of the smooth wall are: Sz = 5.60 µm, Sa = 0.26 µm, and Sq = 0.35 µm.

From the analysis of the motifs presented in Figure 11 below, an average volume of 28.2 µm³ was obtained. Table 1 presents the results of the motifs analysis on the smooth wall.

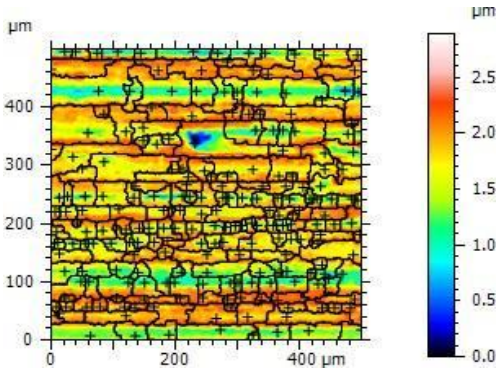

Figure 11. Analysis of motifs on the smooth wall

Table 1. Results from the motifs analysis on the smooth wall

Parameter	Statistic	Value	Unity
Height	Average	0.309	µm
Area	Average	1128	µm²
Volume	Average	28.2	µm³

3.1.2.2. Groove

Figures 12 and 13 below show the profiles of the groove, also traced parallel and perpendicular. In this case, there is a significant difference between both profiles, where the roughness along the parallel profile is more intense. It is worth mentioning that this is the direction in which the fluid flows through the groove along the heat exchanger tube; therefore, this profile may be more significant for potential disturbances.

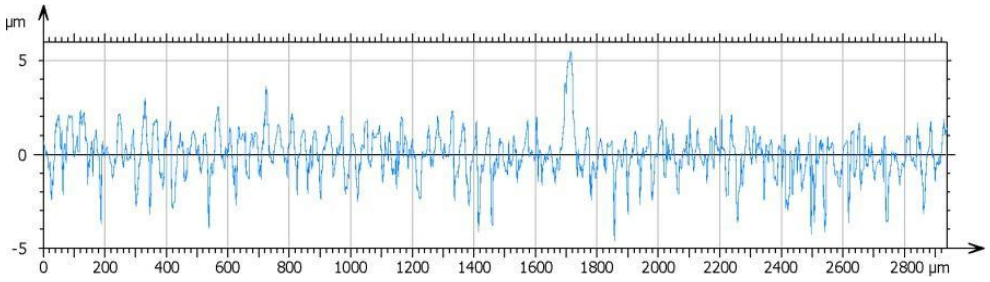

Figure 12. Profile 3, parallel to machining passes

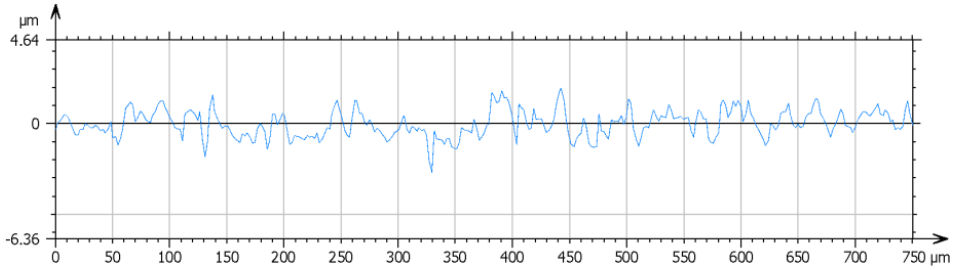

Figure 13. Profile 4, perpendicular to machining passes

In this case, the topographic parameters obtained from the groove data collection were: *Sz* = 19.70 µm, *Sa* = 1.01 µm, and *Sq* = 1.30 µm.

For the groove surface, from the motif analysis presented in Figure 14, an average volume of 97.7 µm³ was obtained. Table 2 presents the results of motif analysis on the groove.

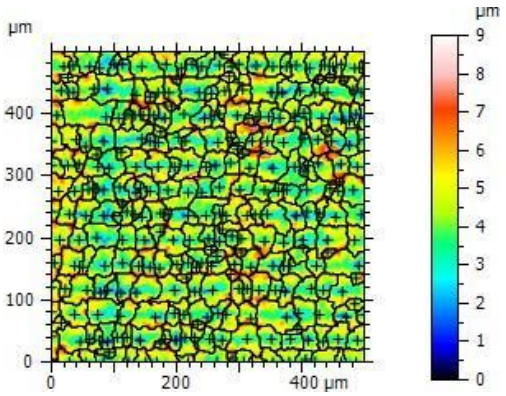

Figure 14. Analysis of motifs on the smooth wall

Table 2. Results from the motifs analysis on the groove

Parameter	Statistic	Value	Unity
Height	Average	1.30	µm
Area	Average	856	µm²
Volume	Average	97.7	µm³

3.2. Solution for thermocouple internal position problem

The implementation of the curved passage rod successfully resolved the challenge of positioning and fixing the thermocouples inside the tubes. In figure 15 (a) and (b) the thermocouples were carefully guided through the gaps by using the rod, which ensured their accurate placement and optimal contact with the inner wall of the tubes. This method allowed for precise temperature measurements, contributing to the reliability and accuracy of the experimental data obtained in the study.

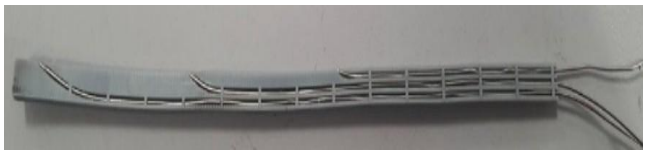

Figure 15 (a). Rod with curved passageways

(b). Tube with inserted rod

4. CONCLUSION

This study demonstrated that the topographic parameters Sa, Sq and Sz in the groove are about four times higher than the smooth tube wall. Additionally, the volume of features in the groove is about three and a half times greater than the smooth wall. In summary, the groove is considerably rougher, which may affect the fluid flow and heat transfer on its surface. In general, a rougher surface can lead to changes in fluid flow patterns, increased pressure drop, and altered heat transfer features. For example, in fluid flow, a rough surface may cause more frictional resistance, resulting in higher energy losses and potentially affecting the efficiency of the system. In heat transfer applications, a rough surface can disrupt the laminar boundary layer and enhance heat transfer due to increased turbulence and larger surface area, potentially improving the cooling performance.

The use of 3D resin printing and the fabrication of the curved passage rod provided an innovative and effective solution for fixing the thermocouples inside the stainless steel AISI 304 heat exchanger tubes. This enabled the researchers to carry out their experiments with confidence and gather valuable data for their work. For future studies we suggest manufacturing a metal rod whenever possible. Although its geometric complexity makes fabrication difficult, the use of metallic material would provide greater durability and integrity for future experiments, allowing for higher temperatures and other fluids to be used. However, precautions should be taken in order to prevent shorts or masked measurements. Furthermore, we suggest an attempt to weld the thermocouples to the inner wall of the tube using the rods as a guide. However, this procedure should be performed with wire thermocouples instead of the sheathed type.

5. REFERENCES

Abed, Azher M. et al. The role of enhancement techniques on heat and mass transfer characteristics of shell and tube spray evaporator: a detailed review. Applied Thermal Engineering, [S.L.], v. 75, p. 923-940, jan. 2015. Elsevier BV.

Aquatech. Desalination: Our Essential Guide to Desalination and the Global Water Crisis. 2019.

Chen, H.; Jebson, R. Factors affecting heat transfer in falling film evaporators. Food and Bioproducts Processing, Elsevier, v. 75, n. 2, p. 111–116, 1997.

Dumpler, Joseph; Huppertz, Thom; Kulozik, Ulrich. Invited review: heat stability of milk and concentrated milk. Journal of Dairy Science, [S.L.], v. 103, n. 12, p. 10986-11007, dez. 2020. American Dairy Science Association. http://dx.doi.org/10.3168/jds.2020-18605

Gourdon, Mathias; Innings, Fredrik; Jongsma, Alfred; Vamling, Lennart. Qualitative investigation of the flow behaviour during falling film evaporation of a dairy product. Experimental Thermal and Fluid Science, [S.L.], v. 60, p. 9-19, jan. 2015. Elsevier BV. http://dx.doi.org/10.1016/j.expthermflusci.2014.07.017

Hou, Hao; Bi, Qincheng; Zhang, Xiaolan. Numerical simulation and performance analysis of horizontal-tube falling-film evaporators in seawater desalination. International Communications in Heat and Mass Transfer, [S.L.], v. 39, n. 1, p. 46-51, jan. 2012. Elsevier BV. http://dx.doi.org/10.1016/j.icheatmasstransfer.2011.08.023

Huang, X.G.; Yang, Y.H.; Hu, P.. Experimental study of falling film evaporation in large scale rectangular channel. Annals Of Nuclear Energy, [S.L.], v. 76, p. 237-242, fev. 2015. Elsevier BV. http://dx.doi.org/10.1016/j.anucene.2014.09.053

Ji, Wen-Tao et al. Falling film evaporation and nucleate pool boiling heat transfer of R134a on the same enhanced tube. Applied Thermal Engineering, [S.L.], v. 147, p. 113-121, jan. 2019. Elsevier BV. http://dx.doi.org/10.1016/j.applthermaleng.2018.10.062

Köroğlu, Batikan; Lee, Kee Sung; Park, Chanwoo. Nano/micro-scale surface modifications using copper oxidation for enhancement of surface wetting and falling-film heat transfer. International Journal Of Heat And Mass Transfer, [S.L.], v. 62, p. 794-804, jul. 2013. Elsevier BV. http://dx.doi.org/10.1016/j.ijheatmasstransfer.2013.03.040

Leheng Chemical Equipment Manufacturing (China). 3T/h MVR Falling Film Evaporator for Ethanol Extract Concentrating.

Lyle, Oliver. The Efficient Use of Steam. London: Her Majesty's Stationery Office, 1947.

Ma, Liangdong; Zhang, Jili; Zhang, Tianjiao. Experimental study on falling film evaporation characteristics of R-134a outside of a vertical enhanced tube. International Journal Of Heat And Mass Transfer, [S.L.], v. 180 dez. 2021.

Ribatski, G.; Jacobi, A. M. Falling-film evaporation on horizontal tubes—a critical review. International Journal of Refrigeration, v. 28, n. 5, p. 635–653, ago. 2005. https://doi.org/10.1016/j.ijrefrig.2004.12.002

Shen, Shengqiang et al. Heat transfer performance and bundle-depth effect in horizontal-tube falling film evaporators. Desalination and Water Treatment, [S.L.], v. 51, n. 4-6, p. 830-836, jan. 2013. Informa UK Limited.

Silveira, Arlan Caldas Pereira. Thermodynamic and hydrodynamic characterization of the vacuum evaporation process during concentration of dairy products in a falling film evaporator. 2015. 179 f. Tese (Doutorado) – Programa de Pós-graduação em Ciência e Tecnologia de Alimentos, Universidade Federal de Viçosa, Viçosa, 2015.

Wang, Qunchang et al. Heat Transfer Characteristics of Falling Film Process on Coated Division Tubes: Effect of the Surface Configurations. Industrial & Engineering Chemistry Research, v. 49, n. 14, p.6622-6629, 21 jul. 2010. American Chemical Society (ACS). http://dx.doi.org/10.1021/ie9018676

Wang, Xianmao et al. Prediction of falling film evaporation on the AP1000 passive containment cooling system using ANSYS Fluent code. Annals of Nuclear Energy, [S.L.], v. 95, p. 168-175, set. 2016. Elsevier BV.

Wuxi Chemical Equipment (China). High-Efficiency Falling Film Evaporator/Reboiler.

6. RESPONSIBILITY NOTICE

The authors are the only responsible for the printed material included in this paper.